Datuming by wavefield depth extrapolation

Jun Ji [1]

ABSTRACT

I present a poststack and a prestack datuming scheme that uses wavefield depth extrapolation. The method I have developed allows the use of any depth extrapolation technique, such as phase-shift, split-step, and finite-difference extrapolation. I derive the datuming algorithms by transposing and taking the complex conjugate of the corresponding forward modeling operator, which does upward extrapolation from a flat surface to an irregular surface. The exact conjugate relation between the forward modeling operator and the datuming operator is demonstrated algebraically. Testing both the poststack and prestack datuming algorithms with synthetic data, using several depth extrapolation algorithms, has shown that the method works well.

INTRODUCTION

Seismic data acquired in areas with irregular topography introduce a numerical problem for migration algorithms that are based on depth extrapolation. Since numerically efficient migration schemes are usually based on depth extrapolation algorithms which allow the extrapolation of a wavefield from a flat surface to another flat surface, datuming is required prior to migration. Datuming is a method of processing to extrapolate a known wavefield at a specified datum of arbitrary shape to another specified datum, also of arbitrary shape. For small differences in elevation and slow velocity variations between the input datum and the output datum, static shifting is a sufficiently accurate datum correction procedure. However, for significant differences in elevations and a more complicated velocity model, the accuracy of the static solution may prove to be insufficient; and a more exact method should be used.

Berryhill (1979, 1984) presented a wave equation datuming scheme for poststack and prestack data using the Kirchhoff integral method. Following his work, various

[1]**email:** Author has no known email address.

forms of the Kirchhoff integral solution to the wave equation have been used by different authors for migration (Wiggins, 1984, Shtivelman and Canning, 1988) and layer replacement (Yilmaz and Lucas, 1986, Berryhill, 1986). The Kirchhoff approach is very expensive and cannot be used for a variable velocity medium.

An elegant and simple technique to correct for the error caused by the static time shift was introduced by the "zero-velocity layer" concept (Beasley and Lynn, 1989). Not only is the static shift required before the migration, but this technique cannot even be applied to the computationally attractive phase-shift algorithms (Gazdag, 1978), because it includes the nonphysical characteristic of zero velocity.

Recently Reshef (1991) presented a depth migration algorithm from irregular surfaces with depth extrapolation methods. His technique can be applied to prestack depth migration algorithms, with no limitations on surface irregularity, complexity of the subsurface structure, or velocity function.

In a previous SEP report (SEP-75), Ji and Claerbout presented a datuming scheme that uses the phase shift algorithm. Even though the algorithm passed the dot-product test, the computation time for the datuming is much longer than that for the forward modeling. This tells us that the algorithm might not be the optimal conjugate. This paper examines the algorithms again and provide a clearer algebraic representation of the datuming using, various depth extrapolation schemes such as the phase-shift (Gazdag, 1978), split-step (Stoffa et al., 1990), and finite-difference methods (**?**). It turns out that the datuming algorithm developed in this paper are the same as the extrapolation algorithm used by Reshef (1991) in depth migration.

POSTSTACK DATUMING

In this paper, the basic strategy for finding a datuming operator is that of first formulating a forward modeling operator and then deriving the corresponding datuming operator by transposing and taking the complex conjugate of the forward modeling operator. For poststack or zero offset sections, the forward modeling is an algorithm that extrapolates the wavefield upward from a flat surface to an irregular surface by the one-way wave equation using half the velocity of the medium. The modeling algorithm is derived so that it can be used with any depth extrapolation technique, including the phase-shift, split-step Fourier, and finite-difference methods.

Forward modeling operator

In forward modeling, the wavefield recorded at each geophone along an irregular surface is the wavefield propagated up to the depth level where the geophones are located. It is necessary to stop the wavefield propagation after recording because the reflection coefficient at surface is almost -1 (**?**). To do so, I formulate the forward modeling operator by propagating the wavefield upward with a filter between extrapolation steps to stop the wavefield propagation where it is recorded. Then all wavefields from all depth levels where the geophones are located are summed together to produce the wavefield along the irregular surface. In order to explain the

algorithm clearly and schematically, I use a simple topography model that has only eight geophone groups on an irregular surface, as illustrated in Figure 1.

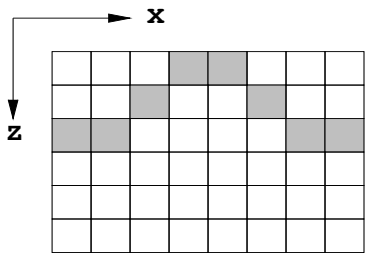

Figure 1: Synthetic surface recording geometry. solid squares represent geophone location on an undulating surface. (syngeometry) [NR]

Figure 2 schematically describes the forward modeling algorithm for the simple model. W_i represents upward extrapolation at the i-th depth level and F_1, F_2, and F_3 are spatial filters for grabbing the wavefield where the geophones are located at the corresponding depth levels. The operators $I-F_3$ and $I-F_2-F_3$ in Figure 2 stop the wavefield at the locations where it is recorded below or at the corresponding depth level and pass the wavefield at the locations where it is not yet recorded. Each small rectangle in Figure 2 represents an abstract vector that contains wavefields at the corresponding space location. The wavefield along the irregular surface is obtained by summing the wavefields that are grabbed at the various depth levels.

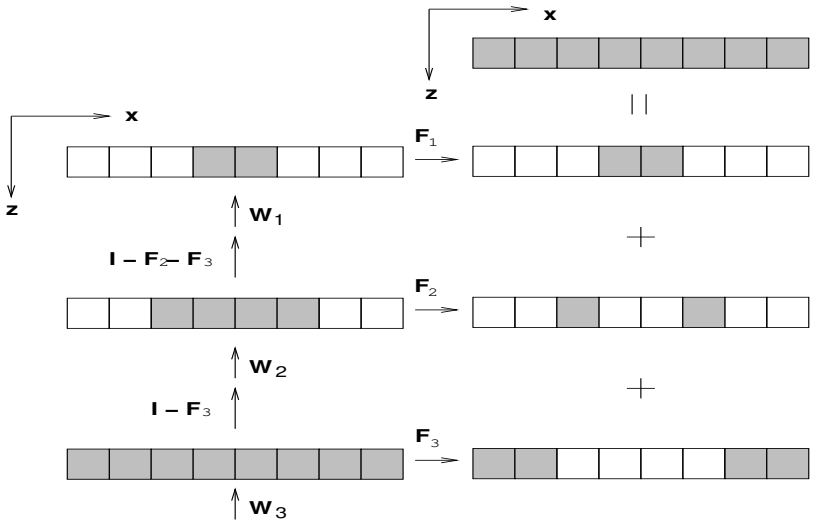

Figure 2: Forward modeling scheme: the schematic diagram for forward depth extrapolation when the surface is not flat. W_i represents the upward extrapolation operator at the i-th depth level. F_1, F_2, and F_3 are spatial filters shown in the text, and I is the identity matrix. (tpfrdschm) [NR]

The forward modeling scheme shown in Figure 2 can be algebraically generalized, if we divide the topography into z levels, as follows:

$$\begin{bmatrix} d_0 \end{bmatrix} = \begin{bmatrix} I & 0 \end{bmatrix} G_1 E_1 G_2 E_2 \dots G_{z-1} E_{z-1} G_z \begin{bmatrix} 0 \\ I \end{bmatrix} \begin{bmatrix} d_z \end{bmatrix} \tag{1}$$

$$E_i = \begin{bmatrix} I & 0 \\ 0 & W_i \end{bmatrix} \tag{2}$$

$$G_i = \begin{bmatrix} I & F_i \\ 0 & K_i \end{bmatrix} \tag{3}$$

where

$$K_i = I - \sum_{j=1}^{z-i} F_{z-j}$$

In equation (1), d_0 and d_z are wavefields on the irregular surface and the datum level, respectively. The extrapolation operator E is followed by the spatial filter G at every depth level. We can see that the upward extrapolation operator W_i is applied to the wavefield that does not arrived at the surface because the operator K_{i-1} remove the wavefield if it has arrived at any previous depth level. All wavefields that arrive at the surface are saved by the operator F_{i-1} for the final output. For the simple geometry shown in Figure 1, F_1, F_2, and F_3 are just diagonal matrices whose elements are 1 where the geophones are located and 0 elsewhere. Thus their diagonal elements are as follows:

$$\begin{aligned} diag(F_1) &= \begin{bmatrix} 0 & 0 & 0 & 1 & 1 & 0 & 0 & 0 \end{bmatrix} \\ diag(F_2) &= \begin{bmatrix} 0 & 0 & 1 & 0 & 0 & 1 & 0 & 0 \end{bmatrix} \\ diag(F_3) &= \begin{bmatrix} 1 & 1 & 0 & 0 & 0 & 0 & 1 & 1 \end{bmatrix} \end{aligned}$$

The operator W_i in equation (2) can be any extrapolation scheme including the Kirchhoff, phase-shift, split-step, or finite-difference method. If we use the phase-shift extrapolation algorithm for W_i, we need an additional inverse Fourier transform in every extrapolation step because the operator G is in the space domain. However, all other algorithms, such as the Kirchhoff, split-step, and finite-difference methods, don't need any additional computation except the operation by G, which is the multiplication of the extrapolated wavefield by the zero/one filter.

Datuming operator

Now the datuming operator can be easily found by transposing and taking the complex conjugate of each matrix in the forward modeling operator shown in equation (1). The datuming operator for a poststack data set gathered on an irregular surface is thus

$$\begin{bmatrix} d_z \end{bmatrix} = \begin{bmatrix} 0 & I \end{bmatrix} G_z^T E_{z-1}^T G_{z-1}^T \dots E_2^T G_2^T E_1^T G_1^T \begin{bmatrix} I \\ 0 \end{bmatrix} \begin{bmatrix} d_0 \end{bmatrix} \tag{4}$$

$$E_i^T = \begin{bmatrix} I & 0 \\ 0 & W_i^T \end{bmatrix} \tag{5}$$

$$G_i^T = \begin{bmatrix} I & 0 \\ F_i & K_i \end{bmatrix} \tag{6}$$

In equation (4), we can see that the downward extrapolation E^T is preceded by the filter G^T at every depth level. We then apply the downward extrapolation operator W_i^T to the wavefield that was introduced by the operator F_i up to a given depth level. The portion of the wavefield that is not introduced until a given depth level is removed by the operator K_i. Figure 3 shows this datuming operator when the topography is given by Figure 1.

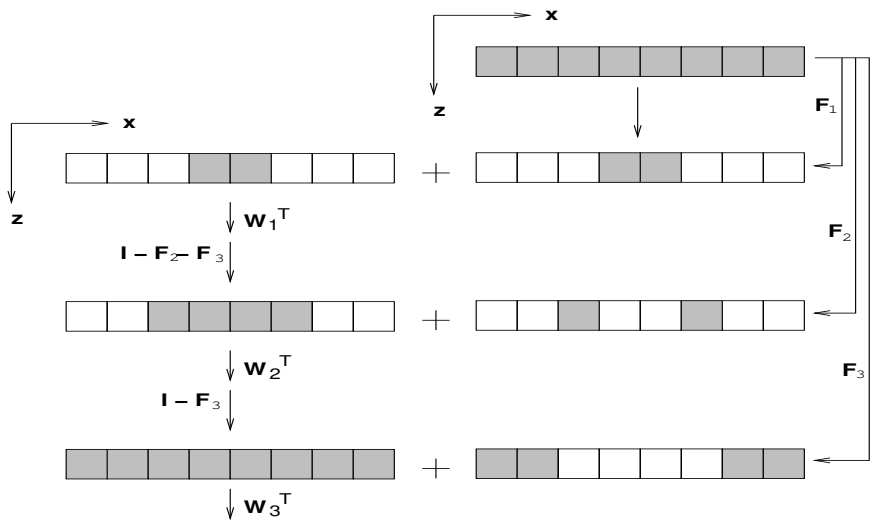

Figure 3: Datuming scheme: schematic diagram for the datuming operator as the conjugate to the forward extrapolation scheme, when the surfaces are irregular. W_1^T represents the downward propagation operator at each depth level. (tpdtmschm) [NR]

Coincidentally, this datuming scheme is the same as Reshef's (Reshef, 1991). He used the algorithm for depth migration from irregular surfaces with depth extrapolation. We can deduce that Reshef's algorithm assumes the same forward modeling algorithm as this one.

Synthetic examples

I test this datuming scheme with phase-shift, split-step, and finite-difference depth extrapolation algorithms. For testing, I use a simple model, Figure 4, that has a syncline reflector under an undulating surface. The irregular surface is modeled to have not only gradual topographic changes but also a discontinuity.

The forward modeling experiment was done using the algorithm explained in Figure 2 for a constant velocity; Figure 5(a) shows the result. Datuming was then

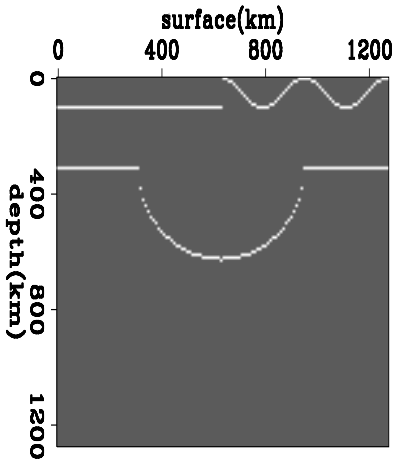

Figure 4: Synthetic model with a syncline reflector image (lower) under an undulating surface (upper). synmdl [R]

performed using the algorithm shown in Figure 3 with the phase-shift extrapolation as the depth extrapolation operator W. The result appears in Figure 5(b); the exact bow-tie shaped wavefield is the characteristic of the syncline reflector on a flat datum. I then applied the same algorithm with the other depth extrapolation schemes. Figures 5(c) and (d) show the datumed results for the split-step and the 45-degree finite-difference methods, respectively. When the velocity is constant, the split-step algorithm is identical to the phase shift algorithm. Therefore we can see that the datumed wavefields in Figures 5(b) and (c) are the same. The result of the finite-difference method, Figure 5(d), also shows a correctly located bow-tie shaped wavefield except very weak artifacts in the region under the undulating surface. These artifacts can be explained as the energy from the evanescent region which has not removed.

To illustrate the effectiveness of the datuming algorithm, a velocity function which varies in depth and lateral extent is tested for the same reflector and topographic model shown in Figure 4. The velocity model used in this experiment has linear increasing both in depth and laterally: $v(x,z) = 1500. + 0.2x + 0.2z$ (Figure 6(a)). The zero-offset data are modeled using split-step extrapolation; Figure 6(b) shows the result. The datuming algorithm is then applied to the data, Figure 6(b), using the split-step extrapolation; the result is shown in Figure 7(a). Figure 7(b) shows the migrated image. By comparing Figure 4 and Figure 7(b) we can see the effect of the datuming algorithm. The datuming algorithm using the finite-difference extrapolation are also tested for the same data Figure 6(b); the datumed wavefield is shown in Figure 7(c) and the migrated image is shown Figure 7(d). In Figure 7(d) we can see the reflector is imaged correctly execpt the steep dip portion, which is limited by the 45-degree wave equation.

Marine data examples

One of the practical applications of datuming in seismic data processing is layer replacement (Yilmaz and Lucas, 1986, Berryhill, 1986). The layer replacement refers

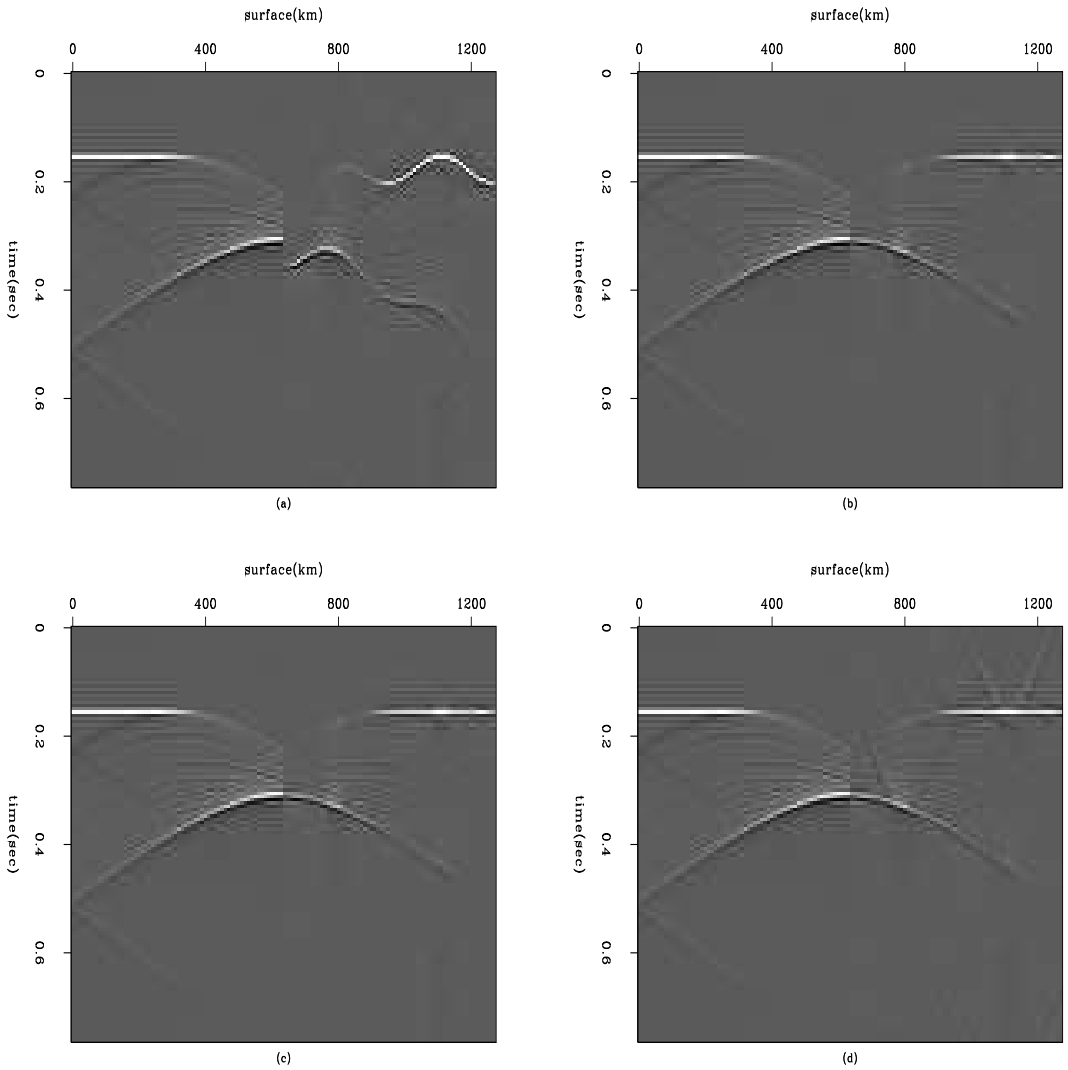

Figure 5: **(a)** Wave field recorded on the irregular surface using phase-shift extrapolation scheme. **(b)** Datumed wavefield using phase-shift algorithm. **(c)** Datumed wavefield using split-step algorithm. **(d)** Datumed wavefield using 45-degree finite-difference algorithm. datumgsw [R]

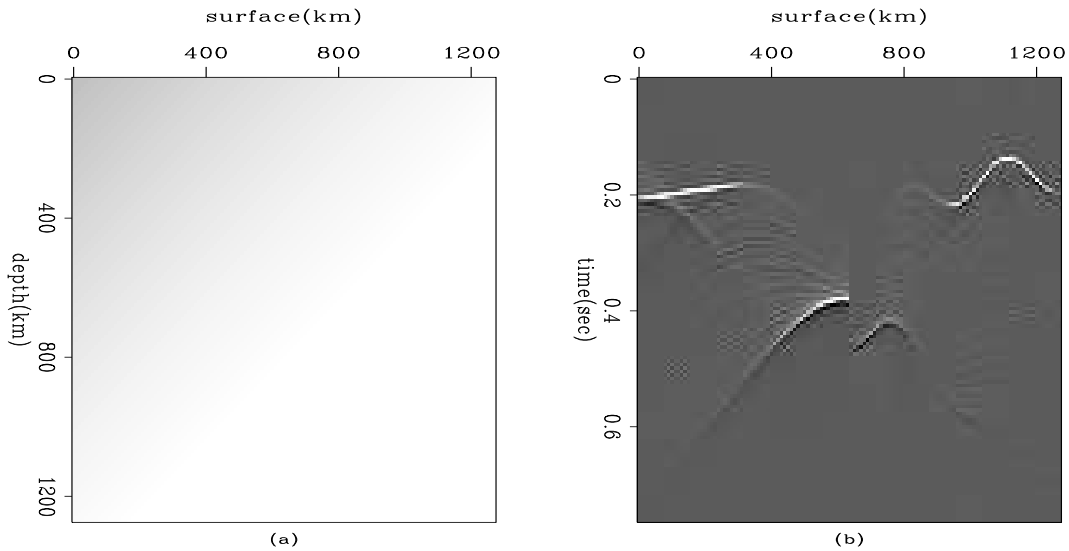

Figure 6: **(a)** velocity model ($v(x,z) = 1500. + 0.2x + 0.2z$). **(b)** Wave field recorded on the irregular surface using split-step extrapolation scheme. vxz-split-modl [R]

to replacing the overburden velocity with the velocity of the substratum, thereby eliminating raypath bendings at the interface between the overburden and the substratum. Time migration after layer replacement can be a practical alternative to depth migration. Therefore, one of the most important things in layer replacement might be preserving the correct spectral property of the original data. The ability to preserve the correct spectral property in layer replacement techniques can be verified by the unitary characteristic of the datuming operator used in the layer replacement.

I applied the datuming algorithm to marine data to illustrate the effectiveness of the datuming algorithm. The near-offset section of a marine data set is displayed in Figures 8. This is the Gulf of Mexico data obtained by Amoco. The complex structure along the sea bottom causes raypath bending that induces distortions and disruptions on reflections beneath a complex structure. The dashed line in Figures 8 represents a datum along the sea floor defined by the first break picks. The near offset is 30 meters so I treat the data as if it were zero-offset and input it to the datuming algorithm.

The datuming to the sea floor is performed using phase-shift extrapolation with water velocity, 1500. m/s, and the result is displayed in Figures 9. To compare with the original data, I used the same water velocity in the process of upward continuing the data back to sea level. Unlike the Kirchhoff datuming (Berryhill, 1979, **?**) which loose some high frequency component, we can see that the datuming used in this paper preserve the spectral property of the original data after layer replacement. The difference between the original data and the data after layer replacement is shown in Figure 11 and confirms the nice property of the datuming operator used.

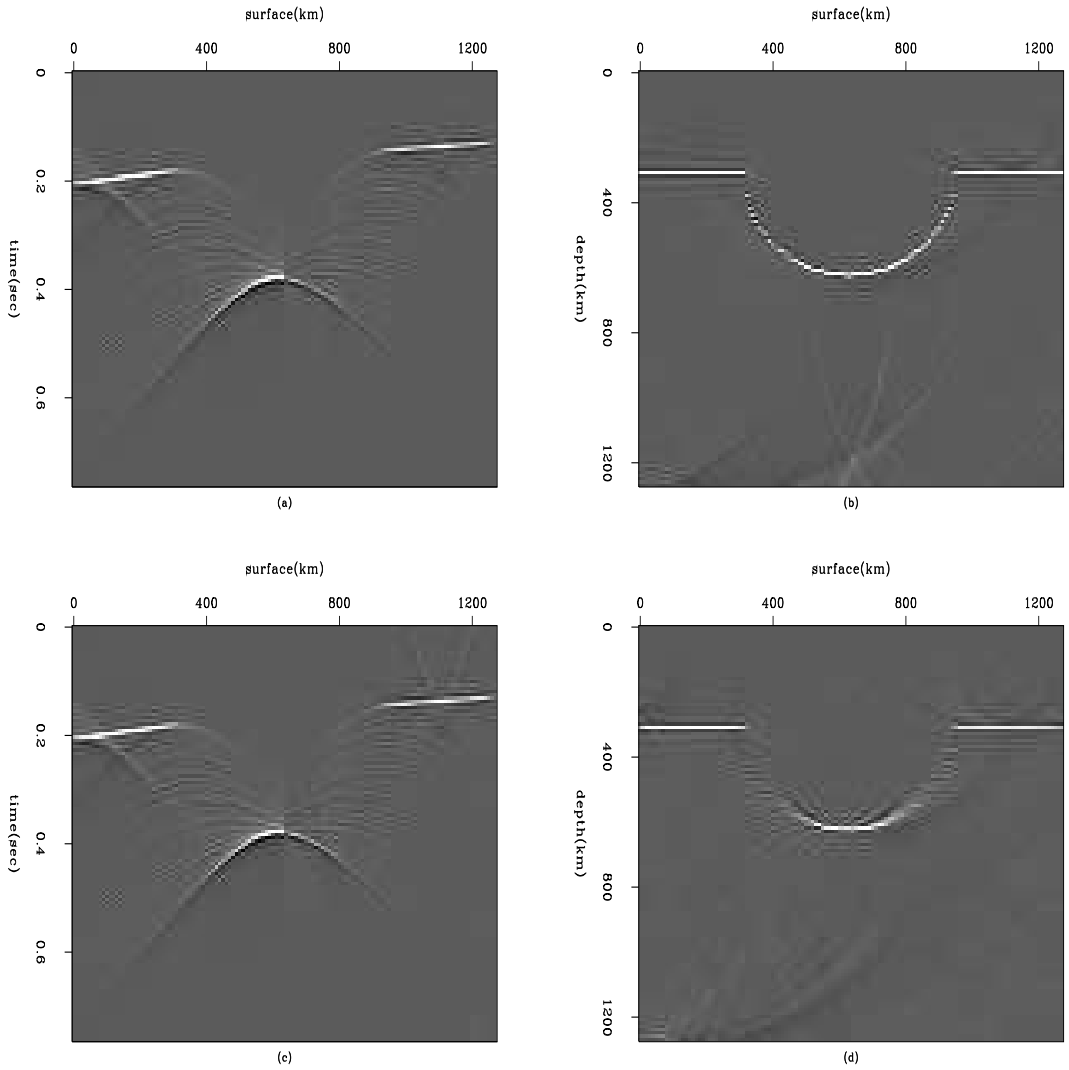

Figure 7: **(a)** Datumed wavefield using split-step algorithm. **(b)** migrated image using split-step algorithm. **(c)** Datumed wavefield using finite-difference algorithm. **(d)** migrated image using finite-difference algorithm. vxz-split-wxz-datum [R]

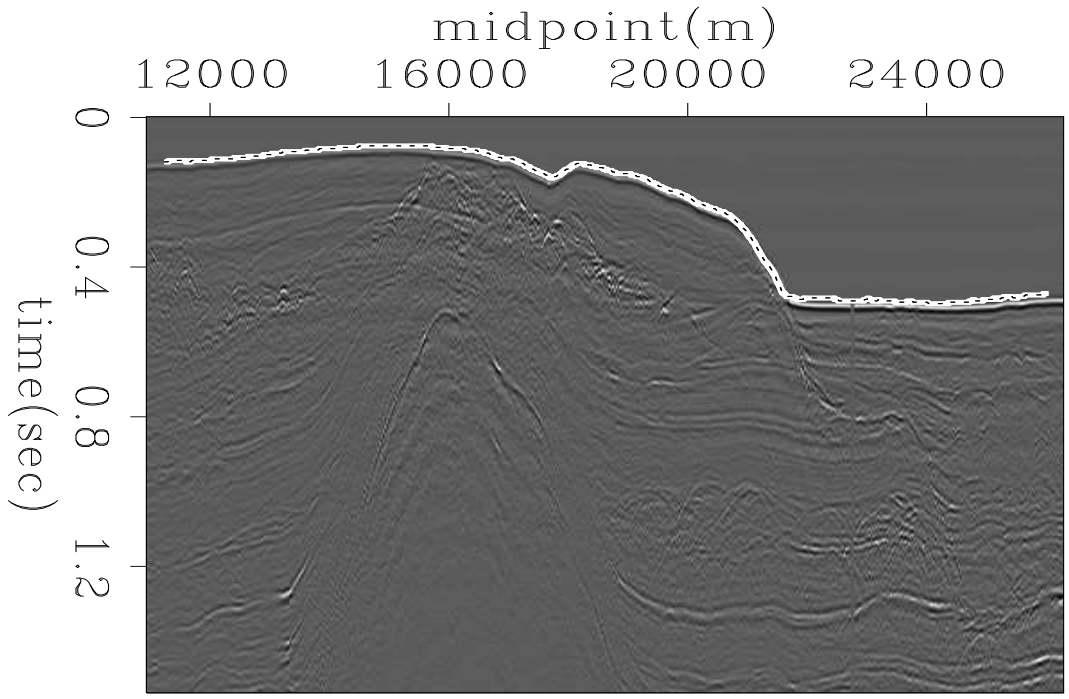

Figure 8: Gulf of Mexico near-offset data with first break picks overlaid. real-data [R]

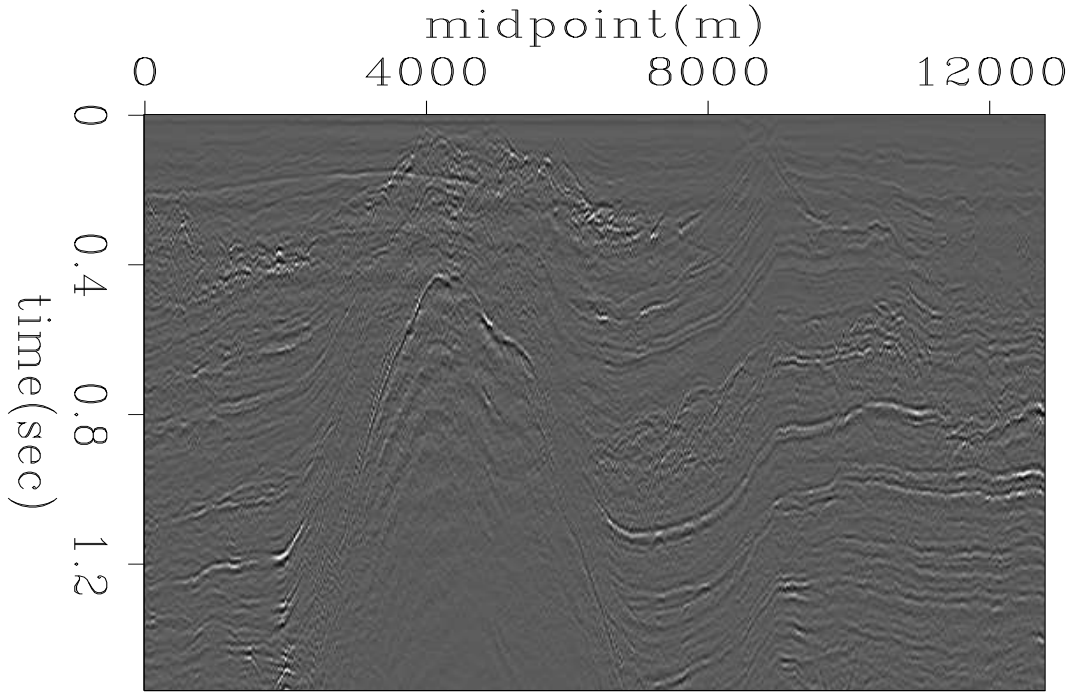

Figure 9: Golf of Mexico near-offset data datumed to the ocean bottom. real-sea-bottom [CR]

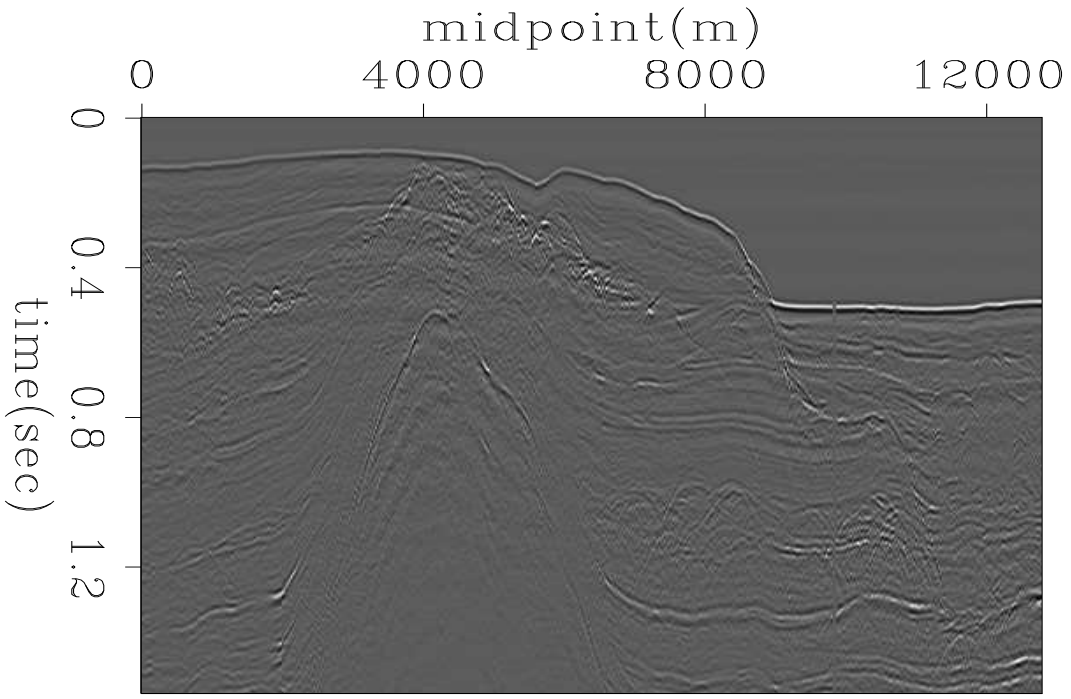

Figure 10: Golf of Mexico near-offset data redatumed to the sea level. real-sea-surface [CR]

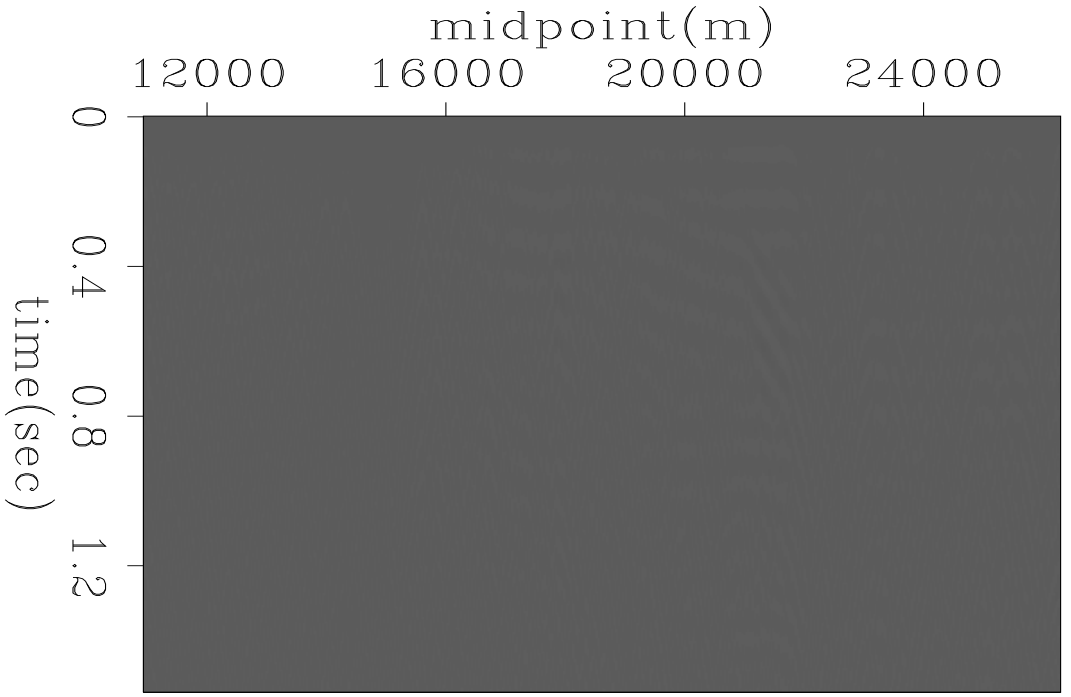

Figure 11: The Difference between Figure 8 and Figure 10. It is too weak to see in the paper printout gray scale. You may try xtpen by clicking the button to see the difference. real-diff [R]

PRESTACK DATUMING

For prestack data, the forward modeling is an algorithm that extrapolates the wavefield upward from a flat surface to an irregular surface by the double-square-root (DSR) equation (**?**). Again, the modeling algorithm is derived so that it can be used with any depth extrapolation technique, including phase-shift, split-step Fourier, and finite-difference methods.

Forward modeling operator

To do forward modeling for a poststack section, we need only consider the locations of geophones. However, in the prestack case, we need to consider the location of both the shots and the geophones, because upward extrapolation using the DSR equation requires both shot and geophone continuation. Thus the spatial filter that stops and keeps extrapolating the wavefield according to the geophone and shot locations becomes more complicated than the filter used in poststack datuming.

The prestack forward modeling can be formulated by propagating the wavefield upward with a filter between extrapolation steps to stop the wavefield propagation after recording for the geophone continuation and after reaching the depth level of each shot for shot continuation. In addition to the filter to stop the wavefield, we need one more operator to save some wavefields that have reached either a shot or a geophone but not the other, for further extrapolation in the corresponding space. Then at all depth levels all wavefields that have reached both a geophone and a shot are summed to produce the prestack wavefield along the irregular surface. In order to explain the algorithm clearly and schematically, I use a simple geometry that has only two geophones and two shots on an irregular surface, as illustrated in Figure 12.

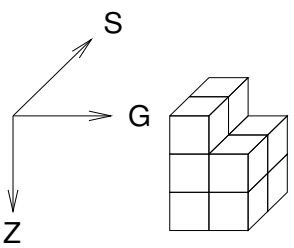

Figure 12: Synthetic surface recording geometry for prestack data. S and G represent the shot and geophone axes, respectively. Z represents depth. (synpretopo) [NR]

Figure 13 is a schematic diagram of the forward modeling algorithm, in which $W_{s,i}$ and $W_{g,i}$ represent upward extrapolation at the i-th depth level for the common-geophone gathers (CGG) and common-shot gathers (CSG), respectively. $K_{g/s,i}$, $H_{g/s,i}$, and $F_{g/s,i}$ are spatial filters for stopping, passing, and grabbing the wavefield at the i-th depth level according to the geophone and shot locations, respectively. Each small rectangle in Figure 13 represents an abstract vector that contains wavefields at the corresponding spatial location.

The forward scheme shown in Figure 13 can be algebraically generalized, if we divide the topography into z levels, as follows:

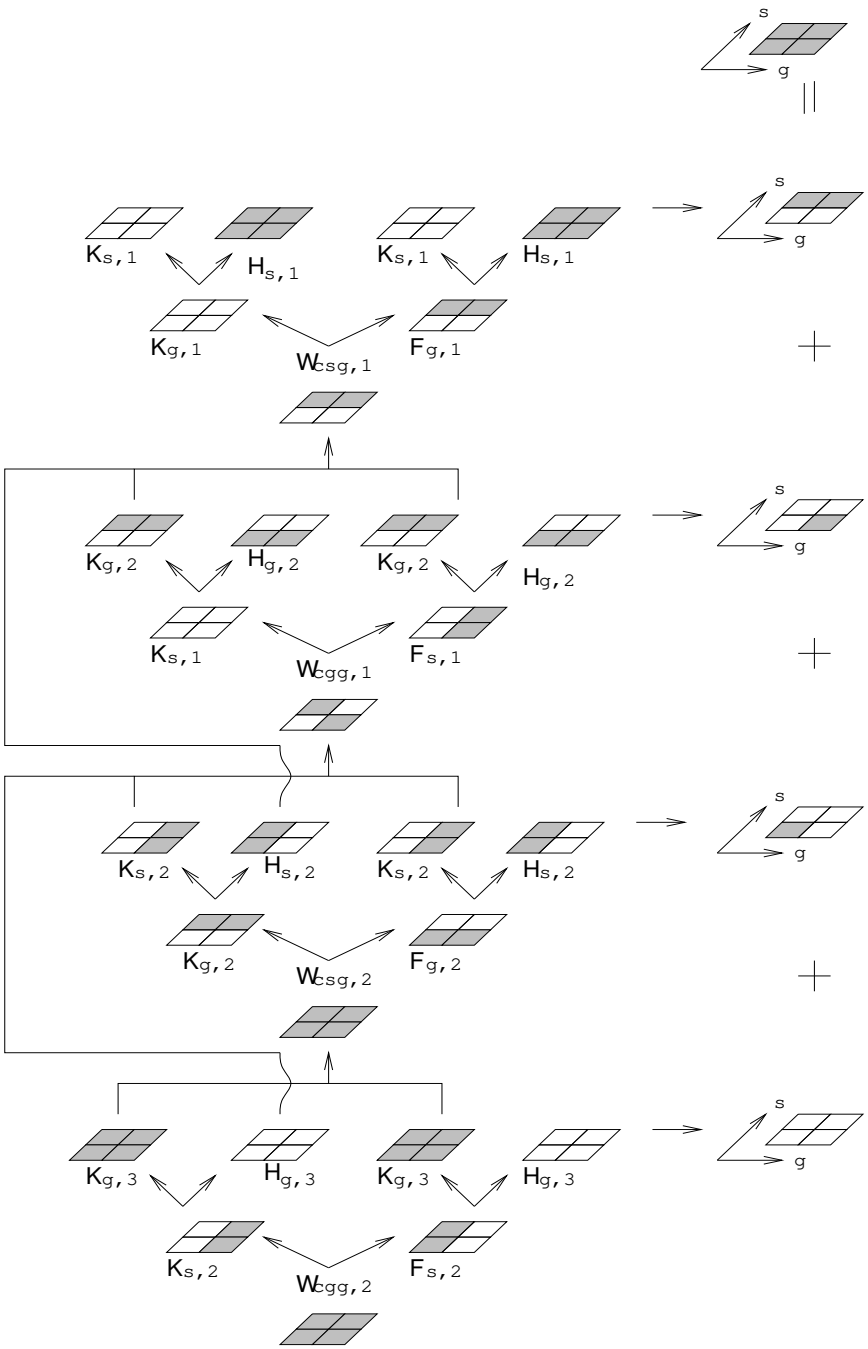

Figure 13: Prestack forward modeling scheme: the schematic diagram for prestack forward modeling when the surface is given by Figure 12. $W_{s,i}$ and $W_{g,i}$ represent upward extrapolation for the common-geophone gathers (CGG) and the common-shot gathers (CSG), respectively, at the i-th depth level. $K_{g/s,i}$, $H_{g/s,i}$, and $F_{g/s,i}$ are spatial filters. The solid and empty rectangles in the filter numerically represent 1 and 0, respectively. (tppremdl) [NR]

$$\left[\begin{array}{c} d_0 \end{array}\right] = \left[\begin{array}{ccc} I & 0 & 0 \end{array}\right] G_{g,1}E_{g,1}G_{s,1}E_{s,1}\ldots G_{g,z}E_{g,z}G_{s,z}E_{s,z} \left[\begin{array}{c} 0 \\ 0 \\ I \end{array}\right] \left[\begin{array}{c} d_z \end{array}\right] \tag{7}$$

$$E_{s,i} = \left[\begin{array}{ccc} I & 0 & 0 \\ 0 & I & 0 \\ 0 & 0 & W_{s,i} \end{array}\right] \tag{8}$$

$$G_{s,i} = \left[\begin{array}{ccc} I & 0 & H_{g,i-1}F_{s,i} \\ 0 & 0 & H_{g,i-1}K_{s,i} \\ 0 & I & K_{g,i-1}(F_{s,i}+K_{s,i}) \end{array}\right] \tag{9}$$

$$G_{g,i} = \left[\begin{array}{ccc} I & 0 & H_{s,i}F_{g,i} \\ 0 & 0 & H_{s,i}K_{g,i} \\ 0 & I & K_{s,i}(F_{g,i}+K_{g,i}) \end{array}\right] \tag{10}$$

where

$$\begin{aligned} H_{s,i} &= \sum_{j=1}^{z-i} F_{s,z-j} \\ K_{s,i} &= I - \sum_{j=1}^{z-i} F_{s,z-j} \end{aligned}$$

In equation (7), d_0 and d_z are wavefields on the irregular surface and the datum level, respectively. The shot extrapolation operator E_s and the geophone extrapolation operator E_g are followed by the shot spatial filter G_s and the geophone spatial filter G_g, respectively, at every depth level. For example, the function of the operator G_s is to sort wavefields into three groups:

- Wavefields that have reached the surface in the shot space among wavefields that have reached the surface in the geophone space. This work is done by the first row of G_s, and the wavefields are saved for the final output.
- Wavefields that have not reached the surface in the shot space among wavefields that have reached the surface in the geophone space. This work is done by the second row of G_s, and the wavefields are saved to be used for the shot extrapolation at the next depth level.
- Wavefields that have not reached the surface in any space. This work is done by the third row of G_s, and the wavefields are saved to be used for the geophone extrapolation use at the same depth level.

The operator G_g works similarly to G_S.

Datuming operator

The datuming operator can now be easily found by transposing and taking the complex conjugate of each matrix in the forward operator shown in equation (7). Thus we obtain the prestack datuming operator for the data gathered on an irregular surface as follows:

$$\begin{bmatrix} d_z \end{bmatrix} = \begin{bmatrix} 0 & 0 & I \end{bmatrix} E^T_{s,z} G^T_{s,z} E^T_{g,z} G^T_{g,z} \ldots E^T_{s,1} G^T_{s,1} E^T_{g,1} G^T_{g,1} \begin{bmatrix} I \\ 0 \\ 0 \end{bmatrix} \begin{bmatrix} d_0 \end{bmatrix} \tag{11}$$

$$E^T_{s,i} = \begin{bmatrix} I & 0 & 0 \\ 0 & I & 0 \\ 0 & 0 & W^T_{s,i} \end{bmatrix} \tag{12}$$

$$G^T_{s,i} = \begin{bmatrix} I & 0 & 0 \\ 0 & 0 & I \\ H_{g,i-1} F_{s,i} & H_{g,i-1} K_{s,i} & K_{g,i-1}(F_{s,i} + K_{s,i}) \end{bmatrix} \tag{13}$$

$$G^T_{g,i} = \begin{bmatrix} I & 0 & 0 \\ 0 & 0 & I \\ H_{s,i} F_{g,i} & H_{s,i} K_{g,i} & K_{s,i}(F_{g,i} + K_{g,i}) \end{bmatrix} \tag{14}$$

Figure 14 is a schematic diagram of the prestack datuming operator when the topography is given by Figure 12. Even though it looks very complicated, the basic algorithm is that which introduces wavefield at each surface location at the corresponding extrapolation level in both the shot and geophone spaces before the shot and the geophone extrapolation and excludes wavefields in the extrapolation in either shot or geophone space if the wavefield was introduced only in the other space.

Synthetic examples

To test the prestack datuming scheme, I used a simple flat reflector with a sinusoidal topography (see Figure 15) and a medium of constant velocity. For the forward modeling, the phase shift extrapolation algorithm was used. The wavefield on the datumed level is shown in Figure 16, and the wavefield on the irregular surface is shown in Figure 17. Figures 16 and 17 show four shot gathers; the location of each shot appears in Figure 15 as a black dot. Because the forward extrapolation used the phase shift algorithm, each shot gather has artifacts caused by the Fourier wraparound. The prestack datuming was performed using the phase shift extrapolation as the depth extrapolation operator W. The four shot gathers after datuming at the same locations as those in Figure 17 are shown in Figure 18. We can see that the datuming operator recovers the hyperbolic event correctly from the hyperbola distorted by the irregular topography. The same prestack datuming algorithm was applied with the finite-difference extrapolation schemes for the whole prestack data

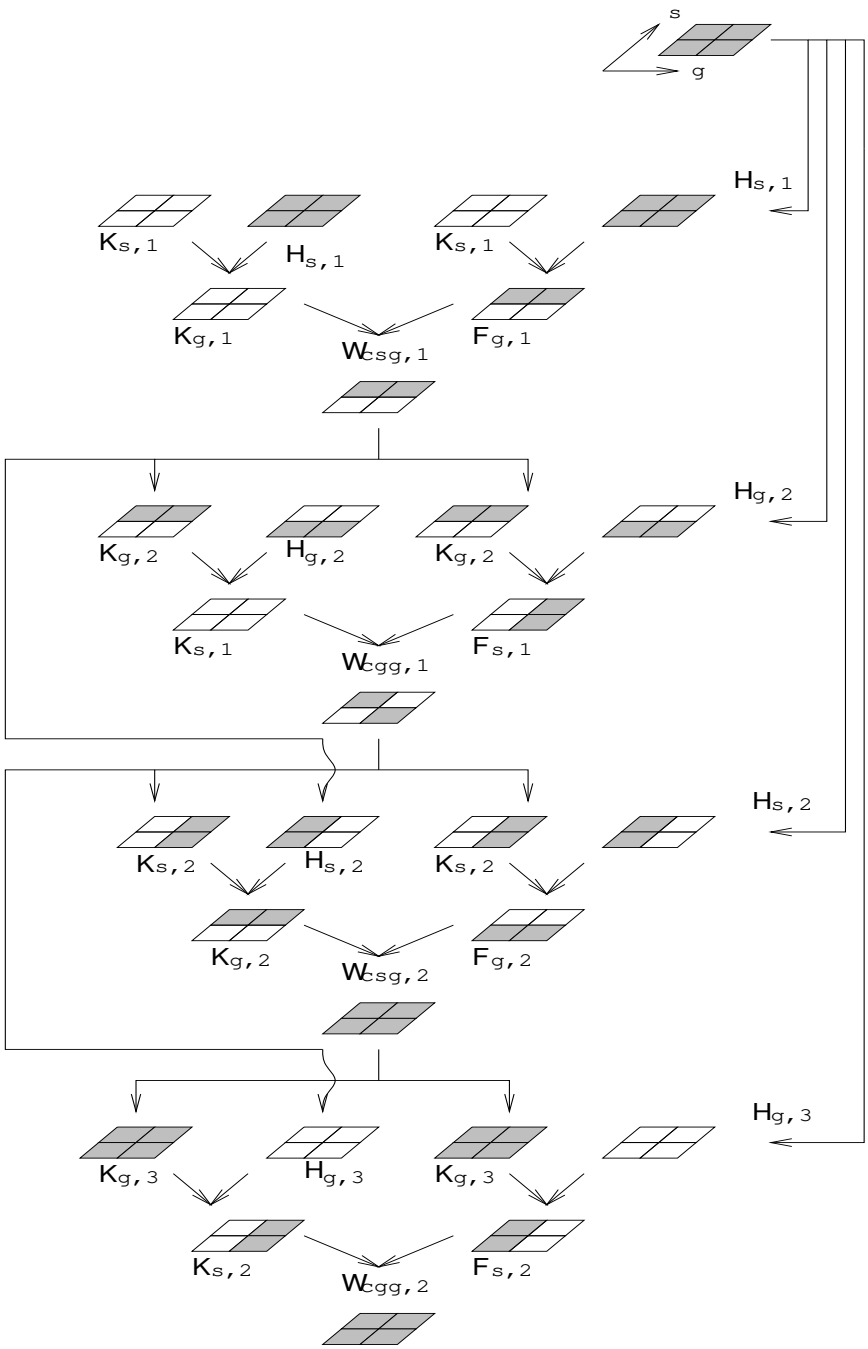

Figure 14: Prestack datuming scheme: The schematic diagram for prestack datuming when the surface is given by Figure 12. $W_{s,i}$ and $W_{g,i}$ represent downward extrapolation for the common-geophone-gathers (CGG) and the common-shot-gathers (CSG), respectively. at the i-th depth level. $K_{g/s,i}$, $H_{g/s,i}$ and $F_{g/s,i}$ are spatial filters. The solid and empty rectangles in the filter represent numerically 1 and 0, respectively. (tppredtm) [NR]

shown in Figure 17; the datumed results appear in Figure 19. The results are also satisfactory.

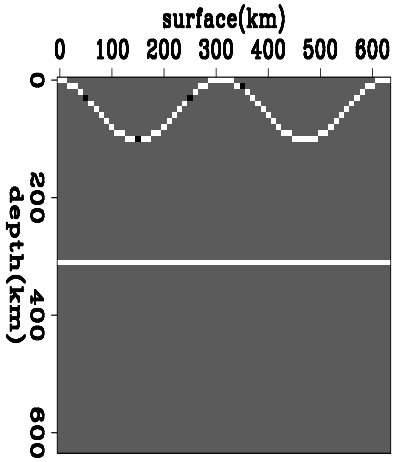

Figure 15: Synthetic model with a flat reflector image (lower) under an undulating surface (upper). Four black dots along the surface represent shot locations shown in Figure 16 presynmdl [R]

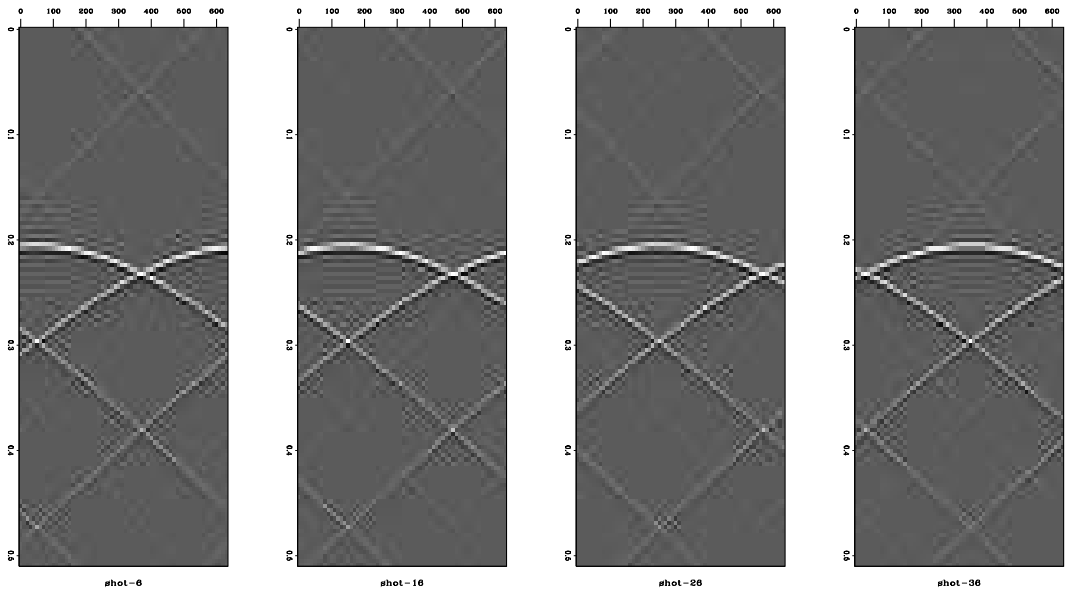

Figure 16: Four shot gathers at the datumed level using the phase-shift extrapolation scheme. csg-at-datum [R]

CONCLUSION

I have developed a poststack and a prestack datuming scheme that use wavefield depth extrapolation. The method allows the use of any depth extrapolation technique such as phase-shift, split-step, or finite-difference extrapolation. The derivation of the datuming algorithms is obtained by transposing and taking the complex conjugate of the corresponding forward modeling operator which does upward extrapolation from a flat surface to an irregular surface. The exact conjugate relation between the

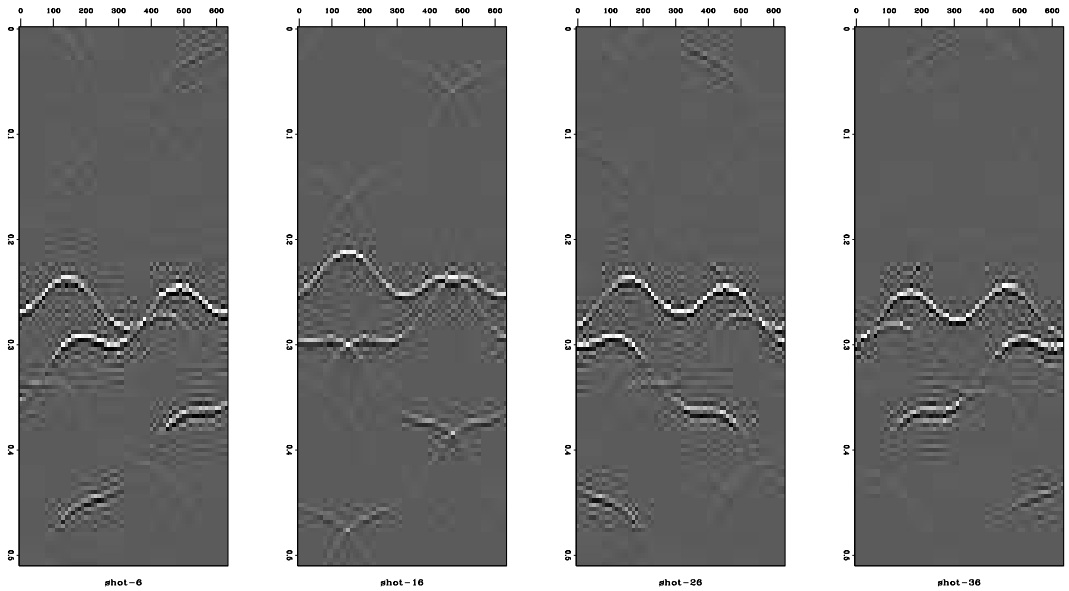

Figure 17: Four shot gathers at the irregular surface using the phase-shift extrapolation scheme. csg-at-surface [CR]

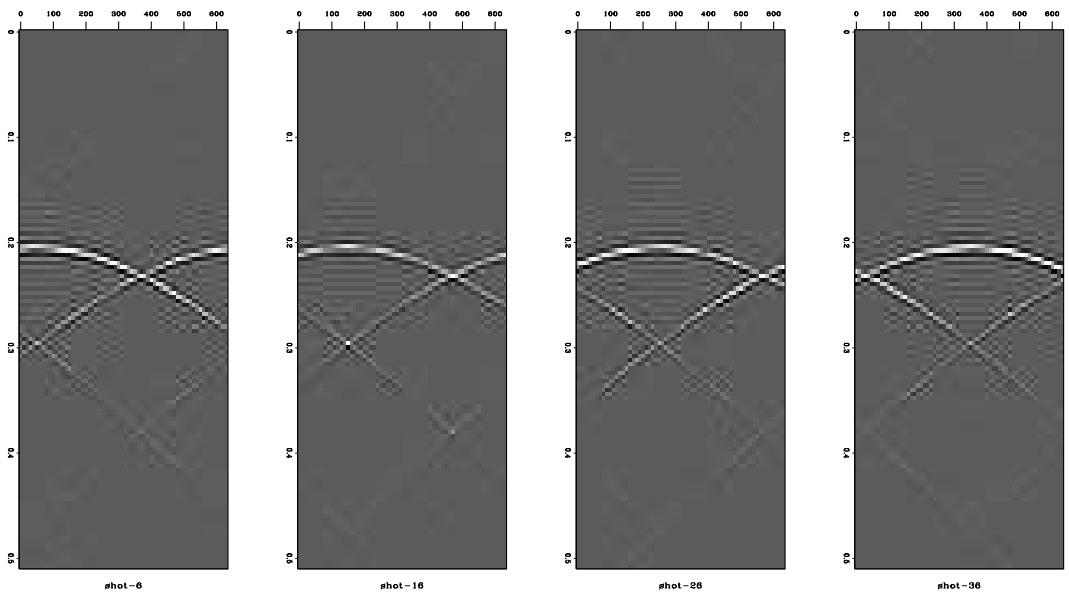

Figure 18: Four shot gathers at the datumed level after prestack datuming using the phase-shift extrapolation scheme. csg-dtmd-gaz [CR]

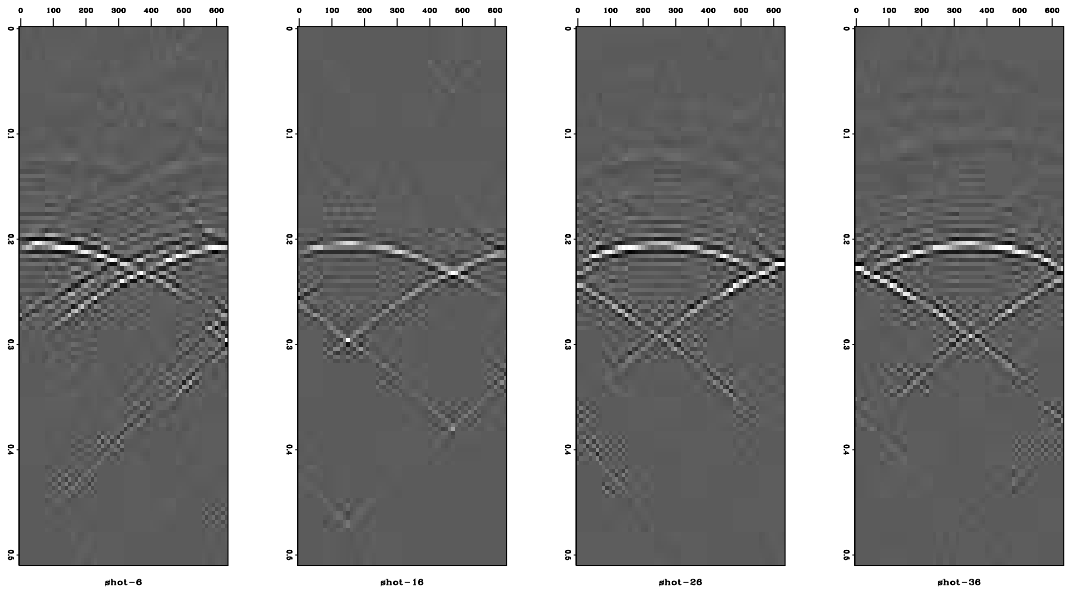

Figure 19: Four shot gathers at the datumed level after prestack datuming using the finite-difference extrapolation scheme. csg-dtmd-wxz45 [CR]

forward modeling operator and the datuming operator is demonstrated algebraically and confirmed by the dot-product test. Several tests of the datuming algorithms with synthetic data and real data show that the method works well.

REFERENCES

Beasley, C. J., and Lynn, W., 1989, Zero-velocity layer: Migration from irregular surfaces: 59th Annual Internat. Mtg., Soc. Expl. Geophys., Expanded Abstracts, 1179.

Berryhill, J. R., 1979, Wave equation datuming: Geophysics, **44**, no. 8, 1329–1344.

Berryhill, J. R., 1984, Wave equation datuming before stack (short note): Geophysics, **49**, no. 11, 2064–2067.

Berryhill, J. A., 1986, Submarine canyons - velocity replacement by wave equation datuming before stack: Geophysics, **51**, no. 8, 1572–1579.

Gazdag, J., 1978, Wave equation migration with the phase-shift method: Geophysics, **43**, no. 7, 1342–1351.

Reshef, M., 1991, Depth migration from irregular surfaces with depth extrapolation methods (short note): Geophysics, **56**, no. 1, 119–122.

Shtivelman, V., and Canning, A., 1988, Datum correction by wave equation extrapolation: Geophysics, **53**, no. 10, 1311–1322.

Stoffa, P. L., Fokkema, J. T., de, L. F. R., and Kessinger, W. P., 1990, Split-step fourier migration: Geophysics, **55**, no. 4, 410–421.

Wiggins, J. W., 1984, Kirchhoff integral extrapolation and migration of nonplanar data: Geophysics, **49**, no. 8, 1239–1248.

Yilmaz, O., and Lucas, D., 1986, Prestack layer replacement: Geophysics, **51**, no. 7, 1355–1369.